Eigenvalue Spectra of Functional Networks in fMRI Data and Artificial Models

Katarzyna Zając and Jarosław Piersa

{zajac,piersaj}[at]mat[dot]umk[dot]pl
Faculty of Mathematics and Computer Science, Nicolaus Copernicus University, Poland

Abstract. In this work we provide a spectral comparison of functional networks in fMRI data of brain activity and artificial energy-based neural model. The spectra (set of eigenvalues of the graph adjacency matrix) of both networks turn out to obey similar decay rate and characteristic power-law scaling in their middle parts. This extends the set of statistics, which are already confirmed to be similar for both neural models and medical data, by the graph spectrum.

Keywords: fMRI, functional networks, neural networks, graph spectrum.

1 Motivation

Recent focus on graph-theoretical description of large-scale real networks caused an avalanche of reports concerning real brain structures and artificial neural networks in this context. Among frequently analysed statistics, degree distribution, transport efficiency, clustering, fault tolerance [3] seem to be most frequently regarded. This seems hardly surprising as they are fairly simple to compute and provide clear conceptual meaning.

In this work we go slightly beyond this classical set of features and focus on the set of eigenvalues of the analysed network (graph spectrum). Such analyses are far less common in theoretical researches concerning ANN[1] and next to absent in experimental neuroscience, though they can still provide a wide qualitative description of the graph, for instance bi-partioning [6]. We provide numerical results concerning spectra of functional graphs from open-accessed fMRI data from BIRN[2] as well as simplified activation-flow of recurrent network. We note a striking similarity between the decay of eigenvalues in functional networks from both sources.

The outline of the paper: in Sec. 2 we describe the methodology and results obtained from fMRI functional graphs. In Sec. 3 we briefly reiterate an

[1] Abbreviations used throughout the paper: ANN — Artificial Neural Network, fMRI — functional Magneric Resonance Imagining, AF — Activation Flow (model), ER — Erdős-Rényi (graph), WS — Watts-Strogatz (graph), AB — Albert-Barabasi (graph)

[2] `http://www.birncommunity.org/resources/data/`

activation-flow model of ANN [13] and recall its spectral properties [14]. The results are compared and discussed in Sec. 4. Sec. 5 concludes the paper and points out potential future research.

2 Spectra of fMRI Functional Brain Graphs

For the study of functional brain graphs, we used fMRI data provided by Biomedical Informatics Research Network (BIRN): we downloaded the data from the open-accessed Function BIRN Data Repository (for more information see the website `http://www.birncommunity.org/resources/data/`). The data contain a raw stream of output of the medical devices, which measured blood-oxygen level in the cells of brain during execution of simple tasks. The fMRI data studied in this paper come from the two-folded run of sensorimotor task, performed by a right handed, non-smoking, healthy women. In Fig. 1 we present the images, which are fragments of obtained scans.

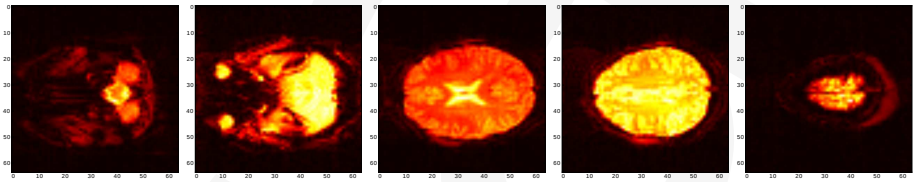

Fig. 1. Representative fMRI scans from the first sensorimotor task at the time $t = 4$ out of 85 timesteps.

The raw data are presented as a set of voxels. Each voxel v, for a given time $t \in \{1, \ldots, n_t\}$, is described by three coordinates $x \in \{1, \ldots, n_x\}$, $y \in \{1, \ldots, n_y\}$, $z \in \{1, \ldots, n_z\}$. By v^t_{xyz} we denote a value of a voxel v with coordinates x, y, z, at a time t. In our analysis we use two datasets. Each dataset consists of 85 three-dimensional data, that represent human brain activity; each volume for a given timestep $t = 1, \ldots, 85$. For a further analysis we use representative fragments of the size $34 \times 40 \times 20$ of volumes imaging human brain, for $t = 1, \ldots, 85$, each frame taken every 3 seconds, so the whole measurement lasted 4:15 minutes.

Based on the fMRI data $D = \{v^t_{xyz} \mid x = 1, \ldots, n_x;\ y = 1, \ldots, n_y;\ z = 1, \ldots, n_z;\ t = 1, \ldots, n_t\} \subset \mathbb{Z}^{n_x} \times \mathbb{Z}^{n_y} \times \mathbb{Z}^{n_z} \times \mathbb{Z}^{n_t}$, we define a *functional activity multigraph* $G = (V, E)$ as follows. For each voxel v, with its coordinates (x, y, z), the *average activity matrix* $A = [a_i] \in \mathbb{M}_{n \times 1}(\mathbb{R})$, where $n = n_x \cdot n_y \cdot n_z$, is defined as

$$A(i := z \cdot n_x \cdot n_y + y \cdot n_x + x) = a_i = \frac{1}{n_t} \sum_{t=0}^{n_t} v^t_{xyz} \ .$$

Using this matrix we define the adjacency matrix of the functional network $Adj = [ad_{ij}] \in \mathbb{M}_{n\times n}(\mathbb{R}_{\geq 0})$, $n = n_x \cdot n_y \cdot n_z$ as

$$Adj(i,j) = ad_{ij} = \begin{cases} |\rho(i,j)| \cdot \sqrt{A(i) \cdot A(j)} & \text{if } |\rho(i,j)| \geq \Theta \\ 0 & \text{otherwise} \end{cases}, \qquad (1)$$

where i and j are the voxel indicates, ρ stands for Pearson correlation coefficient of the activity of the voxels, and Θ is a threshold parameter picked between 0.1 and 1. Fig. 2 depicts fragments of the correlation matrices before thresholding.

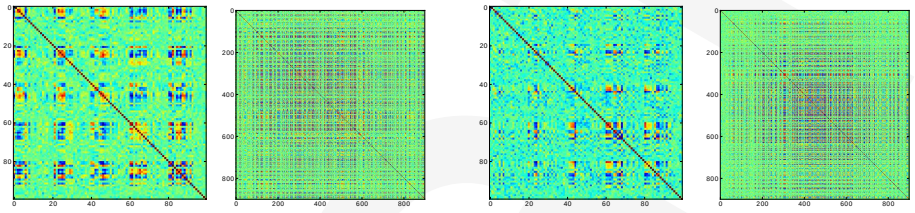

(a) First sensorimotor task (b) Second sensorimotor task

Fig. 2. The fragments of the correlation matrices for the sensorimotor tasks.

We can now proceed to the definition of the functional activity multigraph $G = (V, E)$. The number of the vertices is equal to the number of voxels in D, and each vertex is labelled with coordinates of the corresponding voxel. Between vertices labelled as a and b, there is an edge with a weight equal to $Adj(a, b)$, iff $Adj(a, b) > 0$. Note, that for some thresholds Θ, the obtained graph may not be connected. In that case, as a resulting graph G we assign its maximal connected component, so $|V| \leq n$; see the first two columns of the Table 1 for examples.

The vertex degree distributions of the functional graphs, obtained from described data for thresholds $\Theta = 0.7$ and $\Theta = 0.9$ are given in Fig. 3. We note that they obey a power law formula, which is in agreement with results of Eguiluz et al., see [7], although the threshold values are slightly higher in our case.

We are interested in computing the *spectrum* spec(Adj), that is the set of all eigenvalues of the adjacency matrix:

$$\text{spec } (Adj) = \{\lambda \in \mathbb{C} : \exists_x \in \mathbb{C}^n, \quad \text{such that } Adj \cdot x = \lambda \cdot x\}. \qquad (2)$$

Note that, since the matrix Adj is symmetric, all the eigenvalues are real, i. e. spec $(Adj) \subset \mathbb{R}$, see [6]. The resulting positive eigenvalues were sorted decreasingly and showed in the loglog plots, see Fig. 4. The plots of the spectra for the thresholds $\Theta = 0.3, 0.4, 0.5, 0.6$ are almost overlapping with the results for threshold $\Theta = 0.7$, therefore they are omitted.

The statistics for positive eigenvalues of the resulting graphs are summarized in the Table 1. Interestingly, for larger threshold values the plots exhibit small fluctuation toward developing a power law dependency in the middle part, and

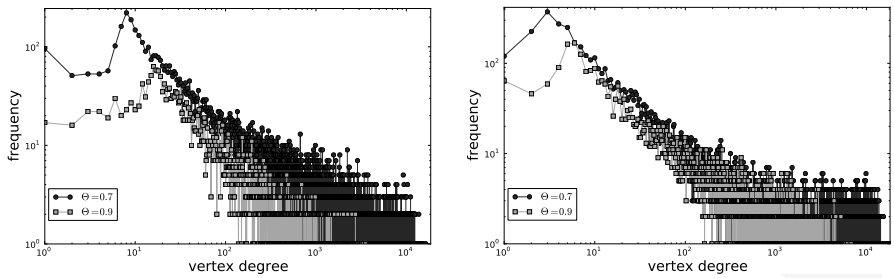

(a) The first task (b) The second task

Fig. 3. Vertex degree distribution of the functional brain network during the sensorimotor tasks for the two thresholds $\Theta = 0.7$, and $\Theta = 0.9$.

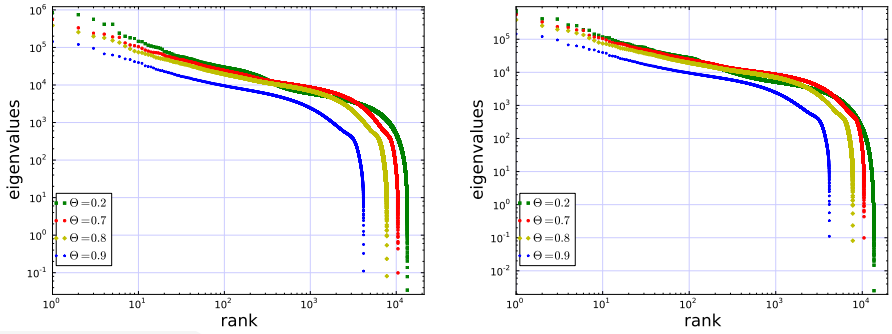

(a) The first task (b) The second task

Fig. 4. Spectra of the functional brain networks during the sensorimotor tasks for various thresholds Θ.

Table 1. Statistics of the positive values of the spectra of the two fMRI datasets (the first and second sensorimotor task, respectively), for varying threshold. Columns from the leftmost denote: threshold, size of the network, minimum eigenvalue, average, median, maximum eigenvalue, variance.

Θ	Size	min	mean	median	max	variance
0.9	3544	0.882	1029.1	533.5	$62.87 \cdot 10^3$	$4.74 \cdot 10^6$
0.8	10545	0.150	1739.5	717.8	$327.43 \cdot 10^3$	$32.30 \cdot 10^6$
0.7	**16435**	**0.199**	**2375.4**	**949.4**	$\mathbf{682.98 \cdot 10^3}$	$\mathbf{85.87 \cdot 10^6}$
0.6	21084	0.029	2879.5	1210.9	$1052.26 \cdot 10^3$	$160.05 \cdot 10^6$
0.5	24541	0.051	3248.5	1489.4	$1413.60 \cdot 10^3$	$250.33 \cdot 10^6$
0.4	26919	0.085	3426.2	1705.5	$1758.03 \cdot 10^3$	$351.79 \cdot 10^6$
0.3	27200	0.000	3580.5	1952.9	$2082.54. \cdot 10^3$	$490.56 \cdot 10^6$
0.2	27200	0.034	3176.1	1577.9	$2372.76 \cdot 10^3$	$599.33 \cdot 10^6$
0.9	6770	0.111	2118.8	779.4	$329.58 \cdot 10^3$	$48.37 \cdot 10^6$
0.8	13268	0.081	3420.0	1255.7	$1268.18 \cdot 10^3$	$272.40 \cdot 10^6$
0.7	**18284**	**0.099**	**3751.7**	**1466.1**	$\mathbf{2107.08 \cdot 10^3}$	$\mathbf{509.93 \cdot 10^6}$
0.6	22184	0.105	3739.1	1512.3	$2746.26 \cdot 10^3$	$698.150 \cdot 10^6$
0.5	24967	0.080	3614.3	1522.9	$3221.10 \cdot 10^3$	$853.56 \cdot 10^6$
0.4	26888	0.011	3343.6	1416.2	$3563.98 \cdot 10^3$	$976.57 \cdot 10^6$
0.3	27200	0.025	3098.1	1337.1	$3799.74 \cdot 10^3$	$1.138 \cdot 10^9$
0.2	27200	0.003	2552.4	907.1	$3950.20 \cdot 10^3$	$1.240 \cdot 10^9$

than truncate exponentially. The segment of this behaviour is quite small but noticeable, especially for $\Theta = 0.7$.

The exact threshold value Θ needs to be adjusted 'manually'. Threshold values selected too strictly may cause removal of vital edges, too generously may preserve unused resources and, in the end, yield a structural, rather than functional graph. In both of the cases the resulting functional network tend to lose its critical properties. Similar loss of criticality outside fixed control parameter was observed in [9], but also fMRI-based researches focus solely on the values, that yield critical state, see for an instance [7].

3 Spectra of Activation-flow-based Model

The prohibitive complexity of the brain dynamics drew us to design a simplified model, which is able to mimic at least some of its characteristic features in the graph-theoretical terms. The activation-flow model, discussed in [13], already turned out to develop a scale-free degree dependency (*ibidem.*) as well as some features, which are typical for the small-world graphs, see [12].

In a nutshell, the model consists of a number of *abstract neurons* $v \in \mathcal{V}$ described by their spatial locations and accumulated *activity* $\sigma_v \in \mathbb{N}_{\geq 0}$. The neurons are connected with symmetric *synapses* with the probability proportional to $|v_1, v_2|^{-\alpha}$, where v_1, v_2 are neurons to be connected, $|-,-|$ is Euclidean distance, and α is a *decay exponent*. We denote the set of synapses by $\mathcal{E}$. Each

connection has its gaussian-drawn *weight* $w_{uv} \in \mathbb{R}$, which indicates its excitatory ($w_{uv} > 0$) or inhibitory ($w_{uv} < 0$) nature. The activity is allowed to be moved between the neurons within following constraints: it cannot be negative ($\forall_{v\in\mathcal{V}} \quad \sigma_v \geq 0$) and its total sum is constant $\sum_{v\in\mathcal{V}} \quad \sigma_v = Const.$ The constant total activity mimics the critical state of the network, so that it neither vanishes nor explodes, see [4]. As a result we can describe the state of the network by its *activity configuration* $\bar{\sigma} = [\sigma_v]_{v\in\mathcal{V}}$. We define an *energy function* $E : \mathbb{Z}^{|\mathcal{V}|} \to \mathbb{R}$ on this configuration space as follows

$$E(\bar{\sigma}) = \sum_{\{v_1,v_2\}\in\mathcal{E}} w_{v_1v_2}|\sigma_{v_1} - \sigma_{v_2}|. \tag{3}$$

If the energy is to be minimized, we can see that two neurons connected with positive weight (excitatory) synapse shall tend to share similar levels of activity, while those connected with inhibitory one ($w_{v_1v_2} < 0$) will prefer high differences in accumulated σ-s (high activity in v_1 silences v_2).

The activity is allowed to flow around the network through synapses according to a stochastic, energy-driven dynamics. At each timestep of the evolution, a single unit of activity is transferred between a pair of neurons, which can be read as a change form configuration $\bar{\sigma}$ to $\bar{\sigma}'$. If such transfer reduces the energy, than it is unconditionally accepted. Otherwise (when $E(\bar{\sigma}') - E(\bar{\sigma}) > 0$) it is accepted with probability exponentially decaying with the growth of the energy. The evolution is run until the network reaches a stable state of the activity configuration, or for a predefined number of time steps. It is not difficult to see relations to the Boltzmann machines dynamics [1], except for adjustments to account for multi-state (rather than binary) neurons. The time-scale of the simulation can be roughly estimated as 10^9 iterations$/(10^4\text{neurons} \cdot 10^3 \frac{1}{s}(\text{spiking frequency})) \simeq 10^2 s$. The estimation is rather crude, but puts the model somewhere nearby the time of fMRI scans, see Sec 2.

Let d_{uv} denote the total number of accepted transfers of activity from u to v, which occurred during the dynamics. Define a *spike-flow* or *functional activity-flow graph* of the system as a subgraph of $(\mathcal{V}, \mathcal{G})$ with multiple edges induced by these synapses of $\mathcal{E}$, which had a vital number of transferred units of activity, that is $\mathcal{G}_1 := (\mathcal{V}, \mathcal{E}_1)$, where $\mathcal{E}_1 = \{e = \{u, v\} \in \mathcal{E} : d_{uv} + d_{vu} \geq \theta\}$, with θ standing for a threshold parameter. Note that, the thresholding parameter θ (lower-case), while has a similar meaning of removal unused resources as in section 2, denoted by capital Θ, but not necessarily the same value and they should not be confused. The edge multiplicities in the functional graphs are equal to the the total activity with flew through the synapse, in other words for $e = \{uv\}$ we have

$$M(e) := \begin{cases} d_{uv} + d_{vu} & \text{if } e \in \mathcal{E}_1 \\ 0 & \text{otherwise.} \end{cases} \tag{4}$$

Recall that the theoretical analyses of spectra for alike model with deterministic winner-take-all dynamics and in full graphs were studied by Schreiber [15], who predicted what i-th principal eigenvalue of the graph should behave as $\frac{c}{i^2}$.

Numerical results concerning of activation flow model were studied in [14] and to some extend confirmed this power law-scaling though with an exponential cut-off of the eigenvalue tail. Interestingly, spectra of recurrent networks with fully connected graph (unlike geometrically-dependent, as in this work) also confirmed similar scaling, but among small number of principal eigenvalues only, see [11].

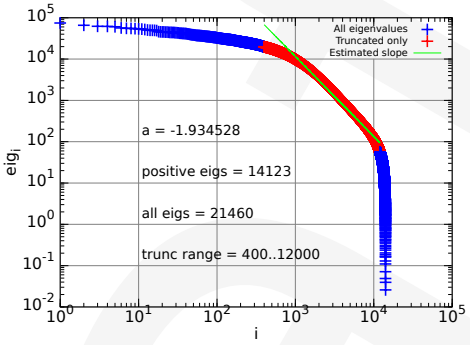

Fig. 5. Log-log plot of the spectrum of the functional graph in activation-flow model, i-th eigenvalue vs i. Eigenvalues are sorted decreasingly. The highlighted middle part of the plot indicates a power scaling ($eig_i \propto i^{-2}$). The network consists of approx. $2 \cdot 10^4$ neurons.

Table 2. Simple statistics of the spectrum of the AF model for varying sample sizes. Columns from the leftmost denote: size of the network (number of neurons), minimum positive eigenvalue, mean, median, maximum eigenvalue, variance.

Size	min	mean	median	max	variance
3048	.133	815.3	256.4	11694.2	$1.7 \cdot 10^6$
3754	.074	960.5	267.3	18015.7	$2.8 \cdot 10^6$
4557	.006	953.2	264.8	13209.6	$2.8 \cdot 10^6$
12530	.040	1962.2	301.6	54041.2	$1.9 \cdot 10^7$
21460	.026	2298.1	287.7	74826.1	$3.3 \cdot 10^7$

The plot of i-th eigenvalue vs. i is depicted in Fig 5. In addition Tab. 2 summarizes the basic statistics of the spectra for various data, though we note, that such statistics can be highly misleading when compared directly. Indeed, entries in adjacency matrix depend of threshold θ and number of transfers d_e, and one might expect that the latter is proportional to the total number of activity in the network (the more total activity is, the more transfers can occur). It is not difficult to see, that if the total sum of σ-s is increased c times than we have: $(Ac) \cdot x = (Ax) \cdot c = (\lambda x) \cdot c = (\lambda c) \cdot x$. So when the initial activity

is multiplied by constant c, than the eigenvalues are also multiplied by c. As a result we conclude that the simple numerical statistics, however interesting, might be deceiving and one should look at the whole shape of the spectrum. In particular, since the power-law-formula distribution X^p, does not have a finite second moment for $p \geq -3$ and even first moment for $p \geq -2$, both mean and variance can be highly misleading statistics.

4 Discussion

Before proceeding to direct comparison we first briefly provide the spectral properties of the best-known graph models, adapted in large scale networks.

First we would like to recall Erdős-Rényi graph model [8], which for a given set of vertices and the probability $p \in (0..1)$ randomly and independently includes each of possible $\binom{n}{2}$ edges into the final graph with probability p: $\mathbb{P}(\{u, v\} \in \mathcal{E}) = p$.

Next random graph to be discussed is a Watts-Strogatz model [16]. Starting from n vertices organized into a ring, each connected with k nearest neighbours, every edge is randomly rewired with probability $p \in [0..1]$. Clearly for $p = 0$ the resulting graph is an unaltered initial periodic lattice, while for $p = 1$ one obtains random ER-graph.

Last of the graph models, to be discussed, was designed by Albert and Barabasi [2]. The construction procedure begins with small clique and iteratively adds new vertices (v_i in i-th step) into the graph, each connected to m existing nodes picked selectively: $\mathbb{P}(\{v_i, u\} \in \mathcal{E}) = \frac{deg(u)}{\sum_{w \in \mathcal{V}} deg(w)}$. The growth is terminated upon reaching desired network size.

Spectra of above reference models are presented in Fig. 6. One should note here, that all the reference models are unweighted single-edge graphs, while the discussed activation-flow model is clearly a multigraph. However, there is a shortage of random graph models, which would account for edge multiplicity.

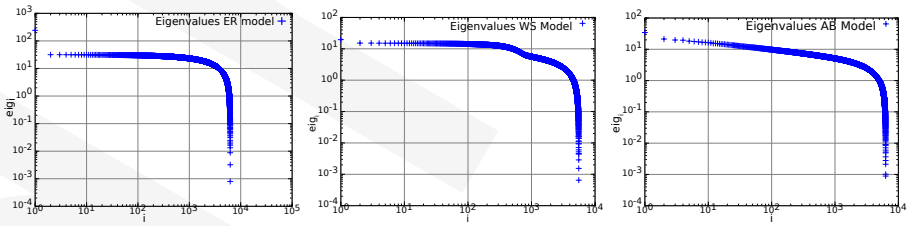

(a) Erdős-Rényi model (b) Watts-Strogatz model (c) Albert-Barabasi model

Fig. 6. Reference spectra of ER, WS and AB random graphs.

Nonetheless, the shapes of the spectra clearly distinct from obtained functional graph in activation flow model as well as fMRI-obtained network. It seems

to be a foregone conclusion in the case of Erdős-Rényi and Watts-Strogatz models, as the obey binomial degree distribution sequences, while the AF model and fMRI turned out to obey a power low decay [13]. The shapes are also different for Albert-Barabasi model, despite the fact that this one is known to reproduce graphs with power law-degree sequences [2]. Interestingly, the fMRI results seem to be able to partially replicate some fluctuations in shape of the Watts-Strogatz spectrum. WS graphs for the probability parameter $10^{-3} < p < 10^{-1}$ are known to be *small-world graphs* (see [16]), but their degree distribution is approximately binomial. We conclude that the obtained spectra are unlike any of the described random graph models, though perhaps random multigraph models would turn out more accurate in predicting.

Instead, as discussed in Section 2, for the threshold value $\Theta = 0.7$ the obtained fMRI functional graphs exhibit a developed power law decay of eigenvalues again in their middle part and than a clear exponential truncation of the eigenvalues. Interestingly, this feature is strikingly similar to one returned by functional graphs of the activation flow model. Somehow unsettling, the segment of validity of such scaling is significantly smaller for fMRI graphs, for the model from Sec. 3 this value was numerically estimated at the 60%, see [14].

Additionally, recall that both functional networks obey a power-law degree distribution, and they share roughly similar way of extraction of the functional network. The statistics, as shortlisted in Tables 1 and 2 follow generally the same tendency, although vary between exact values by even an order of magnitude. However we note that, the power-law distributions may not have finite second or even first moments (see Fig. 7), so one must be careful when inferring just by these values.

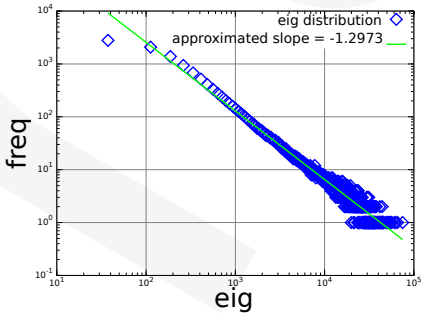

Fig. 7. Empirical distribution of the positive eigenvalues of the model discussed in Sec. 3. Bean lengths are approximately 75 units wide and the plot consists of 1000 beans. Each bean is marked with rhombus, rather than a bar due to log-plot issues. Approximated slope, was fit with least-squares.

5 Conclusion

To conclude, we compared fMRI imagings with artificial model of neural activity in the terms of shape of the eigenvalues of the functional network. We clearly ruled out random graphs of type Erdős and Rényi, Watts-Strogatz or preferential attachment as equivalent model. Instead, the complex dynamics and resource thresholding turn out to be able to reproduce similar results. We still miss an answer whether the power-law scaling should be truncated at some point as the results seem to suggest, or it is just an artefact stemming from small sample size.

In this paper we extend the functional brain network analysis with the spectral properties. Moreover, we compare the spectral properties of functional brain network obtained from freely accessed fMRI data, with artificial models, including activation-flow model, developed in [13]. In the further work it would be interesting to compare the fMRI graph and the functional activity-flow graph in the terms of graph spectral distance (see [10]). Moreover, one can describe the differences between these graphs, using spectral reconstruction techniques, see [5]. This approach can enhance the structure of the functional activity-flow graph to better simulate the behaviour of human brain.

6 Acknowledges

The work has been supported by Ministry of Science and Higher Education research grant DEC-2011/01/N/ST6/01931.

Data used for this study were downloaded from the Function BIRN Data Repository (`http://fbirnbdr.nbirn.net:8080/BDR/`), supported by grants to the Function BIRN (U24-RR021992) Testbed funded by the National Centre for Research Resources at the National Institutes of Health, U.S.A.

References

1. Ackley, D. H., Hinton, G. E., Sejnowski, T. J.: *A Learning Algorithm for Boltzmann Machines*, Cognitive Science, 9(1):147-169, 1985, doi:10.1016/S0364-0213(85)80012-4
2. Albert, R., Barabasi, A. L.: *Statistical mechanics of complex networks*, Reviews of modern physics, Vol 74, January 2002, doi:10.1103/RevModPhys.74.47
3. Bullmore E., Sporns O.: *Complex brain networks: graph theoretical analysis of structural and functional systems*, Nature Reviews, Neuroscience, vol 10, March 2009, doi:10.1038/nrn2575
4. Chialvo, D.: *Critical brain networks*, Physica A: Statistical Mechanics and its Applications, Vol. 340, Issue 4, September 2004, doi:10.1016/j.physa.2004.05.064
5. Comellas, F., Diaz-Lopez, J.: *Spectral reconstruction of complex networks*, Physica A: Statistical Mechanics and its Applications, Volume 387, Issue 25, pp. 6436 - 6442, 2008. doi:10.1016/j.physa.2008.07.032
6. Cvetković, D., Rowlingson, P., Simić, S.: *Eigenspaces of graphs*, Cambridge University Press, 1997

7. Eguiluz, V., Chialvo, D., Cecchi, G., Baliki M., Apkarian, V.: *Scale-free brain functional networks*, Physical Review Letters, PRL 94 018102, January 2005, doi:10.1103/PhysRevLett.94.018102
8. Erdős, P., Rényi, A.: *On random graphs I*, Publ. Math. Debrecen 6, 290–297, 1959
9. Fraiman, D., Balenzuela, P., Foss, J., Chialvo, D. R.: *Ising-like dynamics in large-scale functional brain networks*, Physical Review E, Volume 79, Issue 6, June 2009. doi:10.1103/PhysRevE.79.061922
10. Jovanović, I., Stanić, A.: *Spectral distances of graphs*, Linear Algebra and its Applications, Volume 436, Issue 5, pp. 1425 - 1435, 2012. doi:10.1016/j.laa.2011.08.019
11. Piekniewski, F.: *Spectra of the Spike Flow Graphs of Recurrent Neural Networks*, Artificial Neural Networks - ICANN 2009, 19th International Conference, Proceedings, Part II, 2009, doi:10.1007/978-3-642-04277-5_61
12. Piersa, J.: *Diameter of the spike-flow graphs of geometrical neural networks*, , IX-th International Conference on Parallel Processing and Applied Mathematics; proceedings: Wyrzykowski, R. et al. (Eds.): PPAM 2011, Part I, vol. LNCS 7203, pp. 511–520, Springer, Heidelberg, 2012. doi:10.1007/978-3-642-31464-3_52
13. Piersa, J., Piekniewski, F., Schreiber, T.: *Theoretical model for mesoscopic-level scale-free self-organization of functional brain networks*, IEEE Transactions on Neural Networks, vol. 21, no. 11, November 2010, doi:10.1109/TNN.2010.2066989
14. Piersa, J., Schreiber, T. : *Spectra of the Spike-Flow Graphs in Geometrically Embedded Neural Networks*, proceedings of 11th International Conference on Artificial Intelligence and Soft Computing; L. Rutkowski et al. (Eds.): ICAISC 2012, Part I, LNCS 7267, pp. 143–151. Springer, Heidelberg, May 2012. doi:10.1007/978-3-642-29347-4_17
15. Schreiber, T.: *Spectra of winner-take-all stochastic neural networks*, arXiv [available on-line], `http://arxiv.org/abs/0810.3193v2`, 2010
16. Watts, D., Strogatz, S.: *Collective dynamics of 'small-world' networks*, Nature, vol 393, pp. 440–442, 4 June 1998, doi:10.1038/30918